IET Generation, Transmission & Distribution

Research Article

IET Journals
The Institution of Engineering and Technology

Utilising demand response for distribution service restoration to achieve grid resiliency against natural disasters

ISSN 1751-8687
Received on 10th November 2018
Revised 10th January 2019
Accepted on 14th March 2019
E-First on 24th June 2019
doi: 10.1049/iet-gtd.2018.6866
www.ietdl.org

Faeza Hafiz[1] ✉, Bo Chen[2], Chen Chen[2], Anderson Rodrigo de Queiroz[3,4], Iqbal Husain[1]

[1]*Department of Electrical and Computer Engineering, North Carolina State University, North Carolina, USA*
[2]*Energy Systems Division, Argonne National Laboratory, Illinois, USA*
[3]*Decision Sciences Department, School of Business at North Carolina Central University, North Carolina, USA*
[4]*Civil, Construction, and Environmental Engineering Department, North Carolina State University, North Carolina, USA*
✉ *E-mail: fhafiz@ncsu.edu*

Abstract: The increased frequency of power outages due to natural disasters in recent years has highlighted the urgency of enhancing distribution grid resilience. The effective distribution service restoration (DSR) is an important measure for a resilient distribution grid. In this work, the authors demonstrate that DSR can be significantly improved by leveraging the flexibility provided by the inclusion of demand response (DR). The authors propose a framework for this by considering integrated control of household-level flexible appliances to vary the load demand at the distribution-grid level to improve DSR. The overall framework of the proposed system is modelled as a three-step method considering three optimization problems to (i) calculate feasible controllable aggregated load range for each bus, (ii) determine candidate buses to perform DR and their target load demand, and (iii) maintain the load level in each house through home energy management during the DSR, considering uncertainties in load and solar generation sequentially. The optimization problems are formulated as linear programming, mixed-integer linear programming, and multistage stochastic programming (solved using the stochastic dual dynamic programming) models. Case studies performed in the IEEE 123-node test feeder show improvements in resilience in terms of energy restored compared to the restoration process without DR.

Nomenclature

Indices

t	index for time
l	index for nodes
γ	index for controllable loads
i	house
a, b, c	phases
$\omega_{\mathrm{L},t}$	generated scenario for load
$\omega_{\mathrm{PV},t}$	generated scenario for solar generation

Sets

$\mathscr{L}$	set of all buses in the distribution system
B	set of households in a bus
ϕ	set of phases
$\Omega_{\mathrm{PV},t}$	set of generated scenario for load
$\Omega_{\mathrm{L},t}$	set of generated scenario for solar generation

Parameters

θ_t^{out}	outside temperature at time t
$\underline{\theta_t^{\mathrm{in}}}$, $\overline{\theta_t^{\mathrm{in}}}$	minimum and maximum preferable temperatures inside the house
α, β	thermal parameters of the environment and the appliances in the household
$\underline{P_{\mathrm{ac}}}$, $\overline{P_{\mathrm{ac}}}$	maximum and minimum AC power
Δt	time interval
$\underline{E}$, $\bar{E}$	maximum and minimum washer-dryer energy demands
Q_{b}, Q_{PEV}	capacity of PV-based energy storage and PEV storage
η	efficiency of the charger
$P_{\mathrm{PV},t}$	solar generation at time period t
$P_{\mathrm{load},t}$	load demand at time period t
$\underline{\mathrm{SOC}_t^{\mathrm{B}}}$, $\underline{\mathrm{SOC}_t^{\mathrm{PEV}}}$	minimum state of charge of PV-based energy storage and PEV
$\overline{\mathrm{SOC}_t^{\mathrm{B}}}$, $\overline{\mathrm{SOC}_t^{\mathrm{PEV}}}$	maximum state of charge of PV-based energy storage and PEV
$\underline{P_{\mathrm{b},t}^{\mathrm{ch}}}$, $\underline{P_{\mathrm{PEV},t}^{\mathrm{ch}}}$	minimum charging power of PV-based energy storage and PEV
$\overline{P_{\mathrm{b},t}^{\mathrm{ch}}}$, $\overline{P_{\mathrm{PEV},t}^{\mathrm{ch}}}$	maximum charging power of PV-based energy storage and PEV
$\underline{P_{\mathrm{b},t}^{\mathrm{disch}}}$, $\underline{P_{\mathrm{PEV},t}^{\mathrm{disch}}}$	minimum discharging power of PV-based energy storage and PEV storage
$\overline{P_{\mathrm{b},t}^{\mathrm{disch}}}$, $\overline{P_{\mathrm{PEV},t}^{\mathrm{disch}}}$	maximum discharging power of PV-based energy storage and PEV storage
$\overline{P_{l,t}^{\phi}}$, $\underline{P_{l,t}^{\phi}}$	maximum and minimum demand at each bus at time period t
T	total restoration time period
w_{l}	weight factor of each load
$P_{\mathrm{b},t}$, $P_{\mathrm{f},t}$	base and flexible load at time period t
tf_t	temperature factor
q_t	stochastic parameters
π_t	dual variable
$\mathbb{C}$	controllable bus number

Variables

θ_t^{in}	inside temperature at time period t
$P_{\mathrm{ac},t}$	AC load at time period t
$P_{\mathrm{w},t}$, $P_{\mathrm{d},t}$	washer–dryer load demand at time period t
E_{w}, E_{d}	washer–dryer energy at time period t
$\mathrm{SOC}_t^{\mathrm{B}}$, $\mathrm{SOC}_t^{\mathrm{PEV}}$	state of charge of energy storage and PEV at time period t
$P_{\mathrm{b},t}^{\mathrm{ch}}$, $P_{\mathrm{PEV},t}^{\mathrm{ch}}$	charging power of energy storage and PEV at time period t
$P_{\mathrm{b},t}^{\mathrm{disch}}$, $P_{\mathrm{PEV},t}^{\mathrm{disch}}$	discharging power of energy storage and PEV at time period t
$P_{\mathrm{def},t}$	deferred solar energy at time period t

© The Institution of Engineering and Technology 2019

$P_{g,t}$	load demand from the grid at time period t
μ_t	ratio of flexible and critical load
Γ_i^t	local target load
$P_{l,t}^{\phi}$	load demand in bus l at time period t
$x_{l,t}$	determines whether bus is energised or not{0,1}
y_l	determines whether the bus is controllable or not {0,1}
$\boldsymbol{r}_t$	decision vector

Functions

$h_{t+1}(\cdot)$	recursive function
$\mathbb{E}_{q_{t+1}\|q_t} h_{t+1}(r_t, q_{t+1})$	expected cost function of stage $t+1$
$\|\cdot\|$	represents the cardinality of a set, i.e. the number of elements in that set

1 Introduction

Grid resiliency is essential for future smart distribution systems [1]. To improve grid resiliency, flexibility must be ensured to restore electric service following various post-outage conditions caused by disruptions such as extreme weather and cyber-physical security events. Electric power utilities are paying more attention to grid resiliency and technologies that can reduce the duration of post-disaster outages. Many works have been proposed to improve the resilience metrics by reconfiguring the power system, and improving preparedness for distribution service restoration (DSR). The DSR problem can be formulated as an optimisation problem considering various objectives [2]. In the literature, most studies attempt to maximise load pickup, minimise outage duration, and minimise the number of operations for switches. Some works suggest using synchrophasors [3], reconfiguring networks [4, 5], including distributed energy storage [6], controlling synchronous machine modes [7], curtailing load [8], and using emergency mobile generators [9] during restoration to accomplish these goals. Several works also consider the formation of microgrids by leveraging distributed generators (DGs) and resources during the restoration process [10–18]. In [19, 20], multi-time-step models which can schedule DGs and generate switching sequences for switches are introduced. However, these existing works in the literature did not consider the contribution of demand response (DR) to the restoration procedure.

DR is becoming an integral part of the power system and market operational practice. DR programs have been widely implemented to schedule electricity consumption with the help of advanced metering infrastructure and other smart grid technologies. Several methods of DR have been reported based on various objective functions [21, 22]. For example, an intelligent residential load management system was proposed in [23] for consumers to attain a reduction in electricity bills and maintain the total load under the maximum demand limit by scheduling controllable appliances. A price-based DR of aggregated thermostatically controlled load for load frequency control is suggested in [24]. Wang *et al.* [25, 26], respectively, consider DR and battery storage coordination for load smoothing and reduction of electricity purchase based on time of use rate. Similarly, Huang *et al.* [27] consider social welfare maximisation through dynamic coordination between economic dispatch and DR considering battery energy storage systems (BESSs) and renewable energy resources. Dynamic energy balancing cost model to handle unit commitment and DR are presented in [28–31]. Direct load control (DLC) and load shedding were proposed to minimise power outages during sudden grid load changes to reduce the peak-to-average load ratio [32]. These works did not consider the integration of distribution grid topology with DR, which are proposed in [33, 34]. In [35], a framework is proposed for using DR to provide the capacity release in the distribution system for reliability and risk implications. However, there is no existing work on utilising DR to improve grid resiliency.

This work is concerned with utilising DR to restore loads on unbalanced distribution feeders using a multi-time-step dynamic optimisation model and a microgrid concept with the presence of DGs after a major disaster. Because generation resources can be limited after a major disaster, DR can play an important role in increasing the number of customers served, and/or increasing the total amount of load restored. Because the restoration process may take hours, it is necessary to model the loads as time-varying loads, and hence inter-temporal constraints need to be modelled.

To address these research challenges, this paper proposes to integrate the DR with the DSR framework based on a multi-time-step dynamic optimisation model, which can be applied for radial distribution systems and microgrids with dispatchable DGs. The main contributions of this paper are as follows:

(i) Propose an integrated optimisation framework to coordinate individual operation of flexible residential appliances and the DSR process, so that the benefits of DR in resilience improvement are utilised and quantified.
(ii) Identify operational optimisation models for residential DR and distribution grid restoration considering the interdependent and intertemporal coupling between DR and DSR.
(iii) Provide extensive case studies to verify the effectiveness of the proposed method and quantify the benefits of improving DSR against natural disasters.

The remainder of this paper is organised as follows: Section 2 overviews and introduces the motivation behind the proposed method. Section 3 introduces the hierarchical problem formulation. Section 4 provides the numerical results of a case study, and conclusions are discussed in Section 5.

2 Motivation and proposed method overview

The motivation of utilising DR on a DSR process is shown in Fig. 1 for a three-bus sample distribution system. Two DGs of 20 and 10 kW were supplying two loads, $L1$ and $L2$, which are assumed to be directly connected to the buses. This system can represent a microgrid that is temporarily formed during restoration by sequentially closing the switches and starting the DGs. Fig. 1*a* shows that DG1 and $L2$ are already energised, and DG2 must be started by external cranking power. If $L1$ and $L2$ are fixed-demand loads, $L2$ cannot be restored by closing the switch between bus 2 and bus 3, because this will overload DG1 and the protection may trip DG1 before starting DG2. However, if DR can temporarily reduce the 5 kW load in $L1$, overloading of DG1 can be avoided while restoring $L2$, as shown in Fig. 1*b*. After starting DG2 and having sufficient capacity to support $L1$ and $L2$, $L1$ demand can bounce back to normal demand. In this sense, DR can facilitate releasing capacity constraints and can help ride through some moments when generation (solar, wind etc.) is temporarily insufficient. DR can also temporarily improve the voltage profile until some components with voltage regulation capabilities are energised, such as a voltage regulator, capacitor banks, and dispatchable DGs.

To leverage the flexibility DR provides in a particular bus, the feasible range of load variation should be known for each time period. Feasible range can be calculated considering different types of smart appliances in households that are located in the region served by that particular bus. The two-level control architecture from household appliances to a distribution bus is shown in Fig. 2. If the homeowners are willing to participate in the DR program, they can communicate with the utility regarding the minimum demand considering reduction of some flexible loads like air conditioners, heaters, washers, dryers, solar-based energy storage, plug-in electric vehicles (PEVs), and other loads. To quantify minimum load while still considering the comfort level of the homeowners, we propose an optimisation method to be performed at the household level. The forecasted load demand can be considered the maximum load demand of the household. Because the load forecast is not the primary concern of this work, we assume that the forecasted load is known beforehand. The aggregated maximum and minimum load range for all the houses located in a particular bus can define its feasible range of load demand. This is step 1 in our proposed framework, which is shown in Fig. 3.

© The Institution of Engineering and Technology 2019

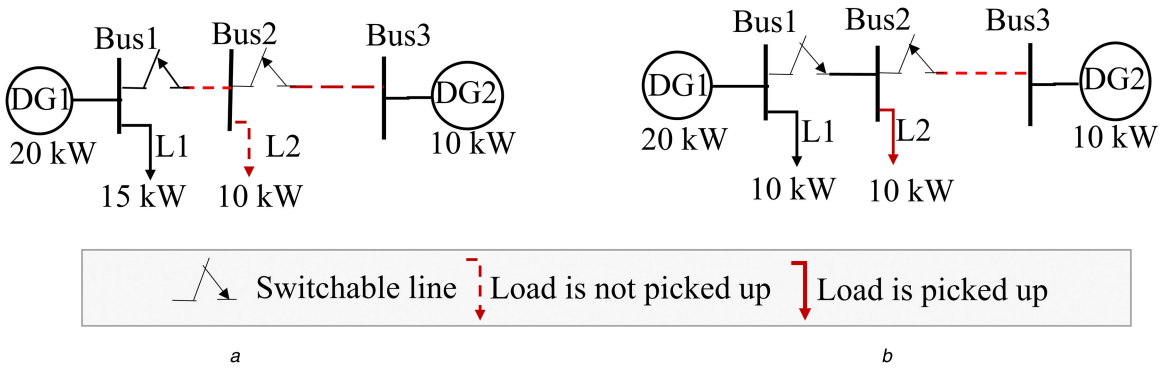

Fig. 1 *Load restoration process of a sample distribution system for*
(a) Fixed load and ***(b)*** Reduced load

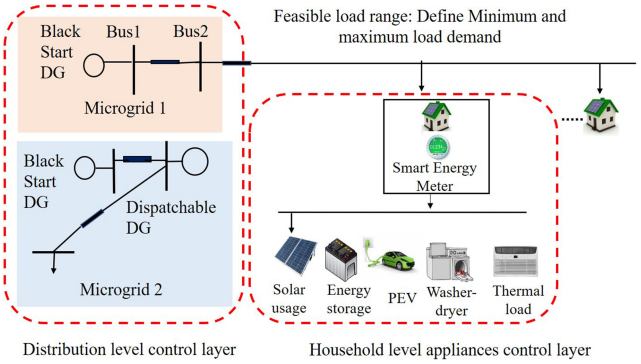

Fig. 2 *Two-level direct load-control-based architecture from household appliances to the distribution system during restoration while microgrids are formed at the distribution level*

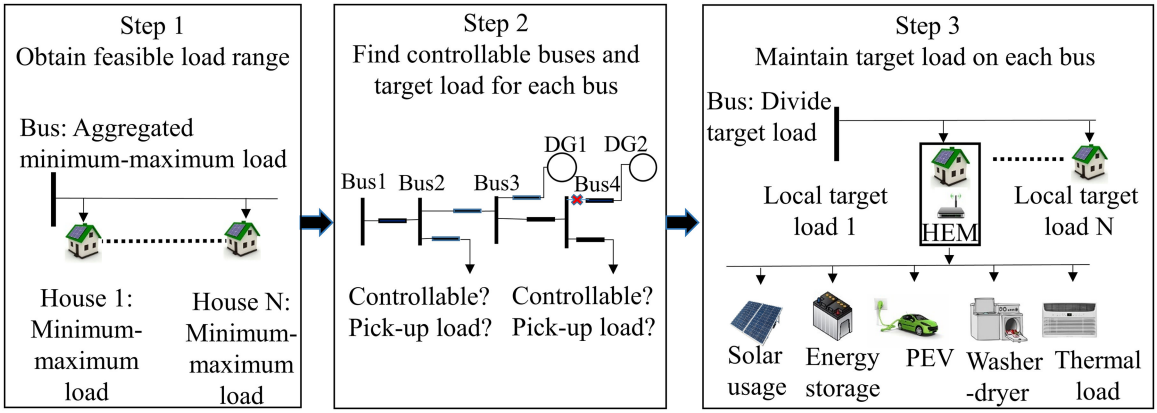

Fig. 3 *Proposed system overview*

In the second step of the proposed framework, we determine whether a bus is energised or not, whether it is controllable or not, and how much load demand will be restored in a particular bus of the distribution level to improve DSR. To obtain answers to these questions, the entire DSR process can be performed through an optimisation process. To make a decision, similar to [20], this optimization process can consider the load variation limit along with the constraints like voltage limit, transformer and line capacity, DG connectivity, DG current unbalance, DG ramp rate, DG output power, load connectivity, and sequencing topology. If only a subset of nodes is selected to provide DR, the proposed optimisation model should find out the optimal selection of the nodes and their corresponding target load profile over the time horizon. This step will define the target load for each bus in the system which is shown in step 2 of Fig. 3.

After obtaining the target load value from the DSR for each bus of the corresponding distribution system, maintaining that load in buses is another issue. This issue can be resolved by scheduling different types of smart appliances at the household level, which is the third step in our proposed framework. The target load obtained from step 2 for a particular bus can be divided among all the existing houses considering their flexible and fixed loads. The divided values can be considered as a local target load for each house. Local target load can be maintained through a home energy management (HEM) system by controlling all of the flexible appliances. In HEM, an optimisation algorithm can be performed to change the original demand of the flexible loads taking into account uncertainty while maintaining their operational constraints and customers' comfort. Because the control is performed considering the uncertainties at the household level to maintain the target, we can treat the load demand as deterministic at the distribution level. Step 3 of Fig. 3 depicts the target load division among houses, and local target maintenance by controlling the smart house appliances in the house.

3 Model formulation

In this section, we introduce three optimisation models corresponding to the three steps introduced in Section 2.

© The Institution of Engineering and Technology 2019

3.1 Optimisation model 1: obtain household-level minimum and maximum load demand requirements over a time period

To evaluate the minimum loads for buses at each distribution level, an optimisation needs to be performed at the household level considering the duration of the restoration process. Day-ahead forecasted load, solar generation, and atmosphere temperature profiles for each household are considered. For DLC, we classify appliances into critical, interruptible, and deferrable loads [36]. Household thermal loads, solar generation, PEV, and energy storage are interruptible loads. Washer and dryers are deferrable loads. Other loads are considered as critical loads for the household.

For thermostatically controlled loads, like ACs and heaters, household owners prefer to maintain indoor temperatures within a bearable range. According to [34], the temperature equations are

$$\theta_t^{\text{in}} = \theta_{t-1}^{\text{in}} + \alpha\left(\theta_t^{\text{out}} - \theta_{t-1}^{\text{in}}\right) + \beta P_{\text{ac},t} \tag{1}$$

$$\underline{\theta_t^{\text{in}}} \le \theta_t^{\text{in}} \le \overline{\theta_t^{\text{in}}} \tag{2}$$

$$\underline{P_{\text{ac}}} \le P_{\text{ac},t} \le \overline{P_{\text{ac}}} \tag{3}$$

Equation (1) evaluates the indoor temperature change. Equations (2) and (3) define the comfortable temperature range for a house and the AC load power range.

Deferrable loads like the washer and dryer depend on energy consumption. The total consumption can be represented as follows:

$$E_{\text{w}} = P_{\text{w},t} \cdot \Delta t \tag{4}$$

$$\underline{E_{\text{w}}} \le E_{\text{w}} \le \overline{E_{\text{w}}} \tag{5}$$

$$E_{\text{d}} = P_{\text{d},t} \cdot \Delta t \tag{6}$$

$$\underline{E_{\text{d}}} \le E_{\text{d}} \le \overline{E_{\text{d}}} \tag{7}$$

where (4) and (6) state the energy consumption of the washer and dryer. Equations (5) and (7) define the maximum and minimum range of energy consumption for the washer and dryer, respectively.

If solar generation and energy storage are available in a house, we use the following equations to consider energy storage control:

$$\text{SOC}_t^{\text{B}} = \text{SOC}_{t-1}^{\text{B}} + \frac{P_{\text{b},t}^{\text{ch}} \cdot \Delta t \cdot \eta}{Q_{\text{b}}} - \frac{P_{\text{b},t}^{\text{disch}} \cdot \Delta t}{Q_{\text{b}} \cdot \eta} \tag{8}$$

$$P_{\text{b},t}^{\text{ch}} \le P_{\text{PV},t} \tag{9}$$

$$\underline{\text{SOC}_t^{\text{B}}} \le \text{SOC}_t^{\text{B}} \le \overline{\text{SOC}_t^{\text{B}}} \tag{10}$$

$$\underline{P_{b,t}^{\text{ch}}} \le P_{\text{b},t}^{\text{ch}} \le \overline{P_{\text{b},t}^{\text{ch}}} \tag{11}$$

$$\underline{P_{\text{b},t}^{\text{disch}}} \le P_{\text{b},t}^{\text{disch}} \le \overline{P_{\text{b},t}^{\text{disch}}} \tag{12}$$

The state of charge (SOC) of the energy storage will change based on the amount of charging and discharging power, which is described by (8). Energy storage will charge from available PV generation based on (9). The maximum and minimum SOC levels of energy storage, and the charging and discharging rate of the charger are defined in (10)–(12).

Similarly, if PEV is available in a house, the storage charging pattern can be controlled considering the upper and lower bounds of the storage and charger rating, which are shown below:

$$\text{SOC}_t^{\text{PEV}} = \text{SOC}_{t-1}^{\text{PEV}} + \frac{P_{\text{PEV},t}^{\text{ch}} \cdot \Delta t \cdot \eta}{Q_{\text{PEV}}} - \frac{P_{\text{PEV},t}^{\text{disch}} * \Delta t}{Q_{\text{PEV}} \cdot \eta} \tag{13}$$

$$\underline{\text{SOC}_t^{\text{PEV}}} \le \text{SOC}_t^{\text{B}} \le \overline{\text{SOC}_t^{\text{PEV}}} \tag{14}$$

$$\underline{P_{\text{PEV},t}^{\text{ch}}} \le P_{\text{PEV},t}^{\text{ch}} \le \overline{P_{\text{PEV},t}^{\text{ch}}} \tag{15}$$

$$\underline{P_{\text{PEV},t}^{\text{disch}}} \le P_{\text{PEV},t}^{\text{disch}} \le \overline{P_{\text{PEV},t}^{\text{disch}}} \tag{16}$$

To include DR, we formulate an optimisation problem to minimise the overall load to purchase from grid. The mathematical model for the optimisation problem for household i is described below:

$$H_i = \min \left\{ \sum_{t=0}^{T} P_{\text{grid},t}^{i} \right\} \tag{17}$$

s.t.:

$$P_{\text{critical},t} + P_{\text{f},t} - P_{\text{PV},t} - P_{\text{b},t}^{\text{disch}} - P_{\text{PEV},t}^{\text{disch}} - P_{\text{def},t} = P_{\text{grid},t}^{i} \tag{18}$$

$$P_{\text{grid},t}^{i} \le 0 \tag{19}$$

where the flexible loads can be defined as

$$P_{\text{f},t} = P_{\text{ac},t} + P_{\text{w},t} + P_{\text{d},t} + P_{\text{b},t}^{\text{ch}} + P_{\text{PEV},t}^{\text{ch}} \tag{20}$$

and constraints from (1)–(16).

Equation (18) is the power balance constraint. Because back-feeding power to the grid may cause overvoltage and safety issues for the grid, we avoid it by maintaining the constraint defined in (19). After solving the optimisation model (1)–(20), we calculate the minimum load requirement from the grid during the restoration process for each household. We account for the maximum load demand by subtracting the forecasted solar generation from the forecasted load demand of the house. To avoid back-feeding power to the grid, negative loads are assumed to be zero and excess solar generation is considered to be deferred energy. Thus, the minimum and maximum loads in bus l are as follows:

$$\underline{P_{l,t}^{\phi}} = \sum_{i \in B} P_{\text{grid},t}^{i} \tag{21}$$

$$\overline{P_{l,t}^{\phi}} = \sum_{i \in B} (P_{\text{load},t}^{i} - P_{\text{PV},t}^{i}) \tag{22}$$

3.2 Optimisation problem 2: calculate distribution-level loads for each bus

For distribution-level optimization problem during restoration, we follow the procedure described in [20]. The proposed sequential service restoration (SSR) method in [20] coordinated all controllable components (e.g. DGs, switchable lines) in the distribution system to restore as much load as possible across multiple steps, and ensured all the distribution-level constraints were satisfied. However, it did not consider coordinated control between load and SSR. Thus, we extend the optimisation model of [20] to pick up as much load as possible during the restoration period by including time-varying flexible load constraints. The objective functions and new load variation constraints are defined below:

$$Z = \max \left\{ \sum_{l \in \mathscr{L}} \sum_{t \in T} \sum_{\phi \in \{a,b,c\}} w_l \cdot P_{l,t}^{\phi} \cdot \Delta t \right\} \tag{23}$$

s.t.:

$$\underline{P_{l,t}^{\phi}} \le P_{l,t}^{\phi} \le \overline{P_{l,t}^{\phi}} \tag{24}$$

$$\overline{P_{l,t}^{\phi}} - M \cdot y_l \le \underline{P_{l,t}^{\phi}} \le \overline{P_{l,t}^{\phi}} + M \cdot y_l \tag{25}$$

$$\begin{aligned} x_{l,t}\underline{P_{l,t}^{\phi}} + (x_{l,t} - x_{l,t-1}) \cdot tf_t \cdot \underline{P_{l,t}^{\phi}} - M \cdot (1 - y_l) \le \underline{P_{l,t}^{\phi}} \\ \le x_{l,t} \cdot \underline{P_{l,t}^{\phi}} + (x_{l,t} - x_{l,t-1}) tf_t \cdot \underline{P_{l,t}^{\phi}} + M \cdot (1 - y_l) \end{aligned} \tag{26}$$

© The Institution of Engineering and Technology 2019

$$tf_t = \frac{(1-\alpha)}{\beta} \tag{27}$$

$$\overline{P^{\phi}_{l,t}} = x_{l,t}\overline{P^{\phi}_{l,t}} + (x_{l,t} - x_{l,t-1}) \cdot tf_t \cdot \overline{P^{\phi}_{l,t}} \tag{28}$$

$$\sum_{l \in L} y_l \leq \complement \tag{29}$$

Other constraints (i.e. system model constraints, system operations constraints, DG operation constraints, connectivity constraints, topological and sequencing constraints) are considered from [20].

Equation (24) considers the time-varying flexible load range on each bus of the distribution system, as calculated in Section 3.1. The big-M method is used in (25) and (26) to ensure that the inequality constraints are applied for controllable buses. Here M is a large number that should be selected carefully. If the load is not controllable, then y_l will become zero. The minimum and maximum loads will be equal to the defined maximum load based on (25); $x_{l,t}$ ensures if a bus is energised or not in (26); and y_l becomes 1 if a bus is controllable. Because maximum load demand is calculated based on the forecasted load demand, this parameter does not consider the temperature impact once it is energized. To include this temperature impact on minimum and maximum load demand just after energising the bus, tf_t is considered in (27), which is calculated based on (1). Thus, (26) shows that if a bus is controllable and it is energised, then the minimum load demand will increase based on the temperature impact during energisation. Maximum load demand of a bus will remain zero until it is not energised. Equation (28) ensures this constraint including the temperature impact on maximum load while bus is energised. Because maximum load demand is calculated based on the forecasted load demand, this parameter does not consider temperature impact. A controllable number of buses can be maintained through (29).

3.3 Optimization problem 3: home energy management (HEM)

The target $P^{\phi}_{l,t}$, which is calculated from Section 3.2 optimisation model, is divided among the houses of each node following the strategy described in [36]. Based on [36], the load is divided among houses considering the aggregated flexible and fixed loads of each house. The following equations are considered for dividing the target $P^{\phi}_{l,t}$ among the houses of each bus:

$$\mu_t = \frac{P^{\phi}_{l,t} - \sum_{i \in B} P^{i}_{b,t}}{\sum_{i \in B} P^{i}_{f,t}} \tag{30}$$

$$\Gamma^{i}_{t} = P^{i}_{b,t} + \mu_t \cdot P^{i}_{f,t} \tag{31}$$

Here Γ^{i}_{t} is the local target load for each house.

If $\mu_t \leq 0$, it can be set as $\mu_t = 0$. In this case, none of the flexible appliances will be turned on in the house to maintain the target load. Only the available amount of supply will be provided to the houses to meet their demand.

If $\mu_t \geq 0$, it can be set as $\mu_t = 1$. In this case, all flexible appliances will be turned on to match the target load in the house.

At the household level, the optimisation model is formulated to maximise the load to purchase from grid, $P^{i}_{\mathrm{g},t}$ by maintaining the target-level electricity demand Γ^{i}_{t} from the grid

$$H = \max \left\{ \sum_{t=0}^{T} \left[P^{i}_{\mathrm{g},t} \right] \right\} \tag{32}$$

s.t.:

$$P^{i}_{\mathrm{g},t} - P_{\mathrm{def},t} = P^{\omega_{L,t}}_{\mathrm{b},t} + P_{\mathrm{f},t} - P^{\omega_{\mathrm{PV},t}}_{\mathrm{PV},t} - P^{\mathrm{disch}}_{\mathrm{b},t} - P^{\mathrm{disch}}_{\mathrm{PEV},t}; \tag{33}$$

$$P^{\mathrm{ch}}_{\mathrm{b},t} \leq P^{\omega_{\mathrm{PV},t}}_{\mathrm{PV},t} \tag{34}$$

$$P^{\mathrm{disch}}_{\mathrm{b},t} + P^{\mathrm{disch}}_{\mathrm{PEV},t} \leq P^{\omega_{\mathrm{L},t}}_{\mathrm{load},t} + P_{\mathrm{f},t} \tag{35}$$

$$P^{i}_{\mathrm{g},t} \leq \Gamma^{i}_{t} \tag{36}$$

and constraints from (1)–(16).

Because load demand and solar generation at the household level are uncertain, the target load demand can be maintained using the scenario generation procedure for these two parameters described in [37]. The power balance equality constraint considering the generated scenario is shown in (33). Equation (34) ensures the charging of storage only from solar generation to reduce electricity purchases from the grid. Equation (35) ensures that back-feeding power to the grid is avoided and thereby to avoid the overvoltage issue. Equation (36) maintains the power demand to the grid up to the target level.

To solve the above maximisation model while considering uncertainties, we decompose and transform it into a T-stage stochastic optimisation model and we apply the Stochastic Dual Dynamic Programming (SDDP) algorithm following the method described in [38]. In the SDDP, the maximum demand is calculated considering future expected demand for each time. To determine the future expected demand, we consider the generated scenario to construct a piecewise linear function through Benders' cuts that are added iteratively at each time stage [38]. The iteration process stops when a stopping criterion is achieved. For simplification, a general T-stage stochastic linear program can be formulated as follows:

$$h_t(r_{t-1}, q_t) = \max_{\boldsymbol{r}_t} \; c_t \boldsymbol{r}_t + \mathbb{E}_{q_{t+1}|q_t} h_{t+1}(\boldsymbol{r}_t, q_{t+1}) \tag{37}$$

s.t.:

$$A_t \boldsymbol{r}_t = B_t r_{t-1} + q_t : \pi_t \tag{38}$$

$$\boldsymbol{r}_t \geq 0 \tag{39}$$

The decision variables of in optimisation model 3.3 in a particular stage t can be considered as the vector defined by $\boldsymbol{r}_t$. Parameter q_t represents the stochastic PV generation and load at stage t. Equation (37) represents the model objective function designed to maximise the total demand, which includes present and expected future demands. Equation (38) represents the power balance, temperature balance, and charge balance constraints in (1), (8), (11) and (33). Dual variables (denoted by π_t) derived from the transition constraints are used later to construct a piecewise linear approximation of the future cost function following Benders' decomposition scheme [38]. Equation (39) represents the simple bounds on the decision variables such as (2)–(7), (9)–(12), (14)–(16), and (34)–(36). For the convergence test, we calculate upper and lower bound demands as described in [38] and consider 95% confidence level criteria. More details about the SDDP algorithm can be obtained in [39–41]. Because the target load is maintained at the residential level considering uncertainties, the distribution load level can be considered deterministic.

4 Simulation results and analysis

4.1 Simulation setup

For simulation, IEEE 123-node test feeder is considered [41]. We introduced four faults and seven DGs in this test feeder to validate the proposed restoration process. Fig. 4 shows the one-line diagram of IEEE 123-node distribution feeder with faults. The three optimisation models are defined as LP, MILP, and T-stage stochastic optimisation model, and are solved using Gurobi optimisation solvers in Python on an Intel Core i7-4600U with a 2-GH CPU, 8 GB of RAM, and 64-bit operating system PC. The restoration time is 8 h using 1-h time interval. Table 1 shows the

© The Institution of Engineering and Technology 2019

parameters of seven DGs. Status '1' indicates a black start DG and '1/0' indicates a non-black start DG.

We downloaded household load profiles and historical temperature dates from Pecan Street [42] and historical climate data of the United States [43], respectively. From [42], we imported the detail load profiles for each electrical appliance and solar generation profiles. For a household, we control the AC load, washer, dryer, PV-based storage, and PEVs optimally to restore the overall load of the grid for an 8-h restoration period. Residential appliance parameters considered for simulation are provided in Table 2. To maintain the spot load level of each bus defined in [44], we assigned the number of houses in each bus in such a way that the highest value in the maximum aggregated load profile did not go beyond that level. Suppose 40 kW spot load at bus number 16 was assigned in [44]. We assigned ten houses in this bus so that the highest value of the maximum aggregated load profile did not go beyond 40 kW. The simulation results with the proposed method were compared with the results for the system where DR was not applied (this analysis is defined as without DR method later in the paper).

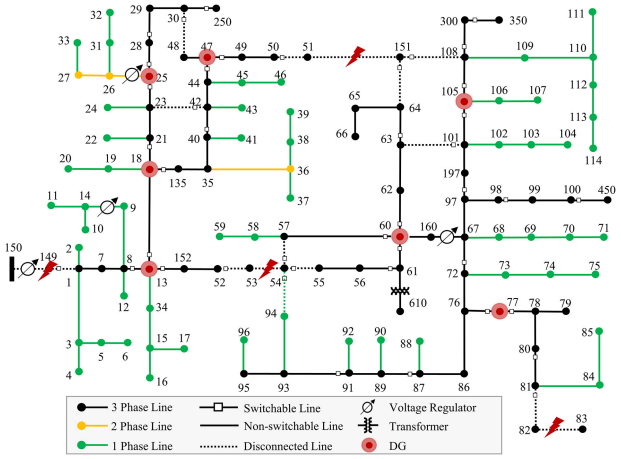

Fig. 4 *IEEE 123-node distribution feeder with faults*

4.2 Effect of DR to improve system resilience

(i) *Without DR*: For comparison, we consider the method described in [20], where DSR is implemented considering loads remain unchangeable. In another word, we can call it a system without DR for our convenience. If the load demands are not controlled with DR in [20], Fig. 5 shows that some buses are not energised. This occurs due to the voltage violation with limited DG capacity compared to the load demands. Voltage violation is a constraint during the restoration of the optimisation model defined in (20) in [20].

(ii) *With DR in the system:* In our proposed approach, we consider the loads are changeable within certain ranges and this change will be implemented through DR. Based on our proposed method, number of preferable controllable buses can be defined. From simulation result, it is found that for 20 controllable buses, all the buses in the distribution are energised. It is as visible in Fig. 6. Locations of the 20 preferred controllable buses are selected using our proposed optimisation method. Other buses are picked up as unchangeable loads. Fig. 7 shows that, overall, 20% more energy restoration is possible with 20 controllable buses, compared to the without DR restoration method. Optimal load profiles for all the buses were obtained from the solution of optimization model (23)–(28) that is maintained through the application of HEM. HEM is described later in Section 4.5.

4.3 Effect of optimal selection of buses with DR participation

Fig. 8 shows the effects of random and optimal location selection of controllable buses. It illustrates that location selected using our proposed method ensures more energy restoration than random selection. It also reveals that with the increase in controllable buses, energy restoration increases. After a certain number of controllable buses, energy restoration becomes saturated. This saturation point can be considered as the 'optimal controllable bus

Table 1 Parameters of DGs added to IEEE 123-test feeder

Parameters	DG1	DG2	DG3	DG4	DG5	DG6	DG7
bus position	13	18	25	47	60	77	105
maximum power, MW	0.9	1.05	1.2	1.5	1.2	0.8	0.7
minimum power, MW	0	0	0	0	0	0	0
maximum reactive power, MVar	0.7	0.8	0.5	0.5	0.4	0.3	1.2
minimum reactive power, MVar	−0.5	−0.5	−0.5	−0.5	−0.6	−0.3	−0.9
status	1	1	1/0	1/0	1	1/0	1

Table 2 Residential appliance parameters

Parameters	Values
$\underline{\theta_t^{\text{in}}}$, $\overline{\theta_t^{\text{in}}}$	72, 78°F
α, β	0.9, −5
$\underline{P_{\text{ac}}}$, $\overline{P_{\text{ac}}}$	0, 5 kW
$\underline{E_{\text{w}}}$, $\overline{E_{\text{w}}}$	0, 2 kW
$\underline{E_{\text{d}}}$, $\overline{E_{\text{d}}}$	0, 2 kW
$\underline{P_{\text{b},t}^{\text{ch}}}$, $\overline{P_{\text{b},t}^{\text{ch}}}$	0, 2 kW
$\underline{P_{\text{b},t}^{\text{disch}}}$, $\overline{P_{\text{b},t}^{\text{disch}}}$	0, 2 kW
$\underline{P_{\text{PEV},t}^{\text{ch}}}$, $\overline{P_{\text{PEV},t}^{\text{ch}}}$	0, 2 kW
$\underline{P_{\text{PEV},t}^{\text{disch}}}$, $\overline{P_{\text{PEV},t}^{\text{disch}}}$	0, 20 kW
Q_{b}, Q_{PEV}	4, 85 kWh
$\underline{\text{SOC}_t^{\text{B}}}$, $\overline{\text{SOC}_t^{\text{B}}}$	20, 80%
$\underline{\text{SOC}_t^{\text{PEV}}}$, $\overline{\text{SOC}_t^{\text{PEV}}}$	20, 80%
η	92%

© The Institution of Engineering and Technology 2019

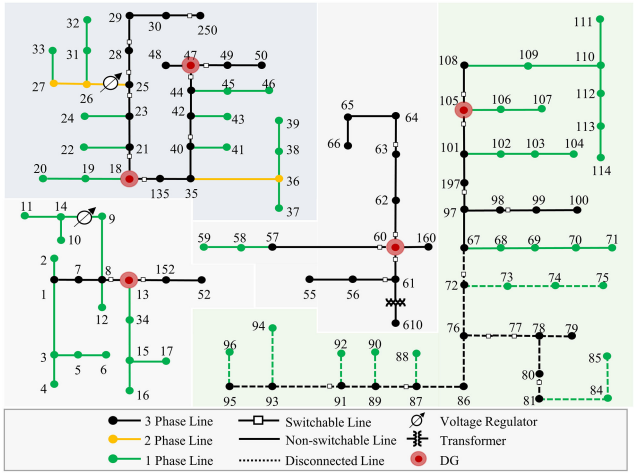

Fig. 5 *IEEE 123-system representation where some buses are not energised if loads are not controllable*

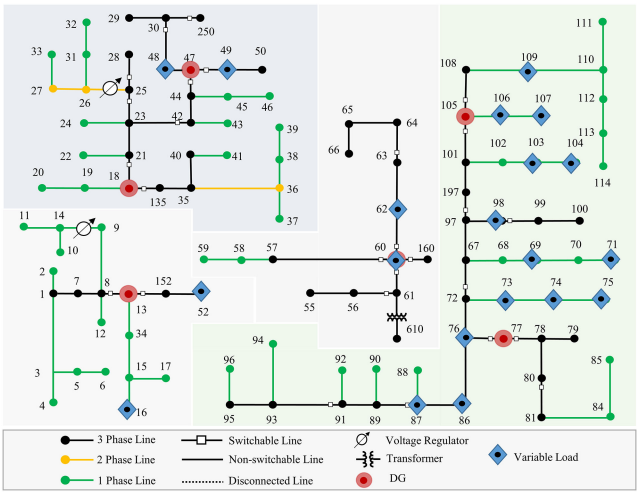

Fig. 6 *IEEE 123-system where all buses are energised by controlling loads of 20 buses within the restoration time*

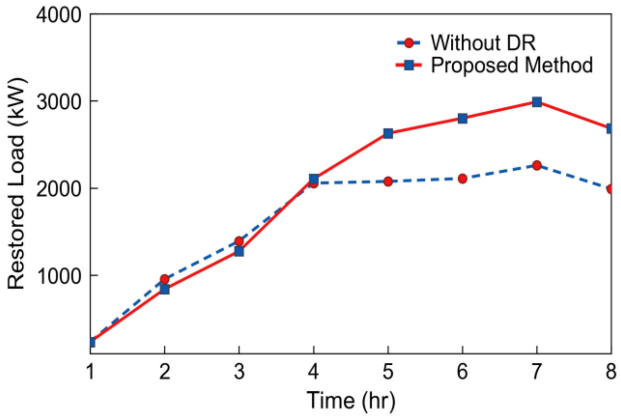

Fig. 7 *Comparison between load restoration at each hour interval without DR and DR based proposed methods with 20 controllable buses*

number'. According to Fig. 8, 'optimal controllable bus number' is 20 for the studied outage condition.

4.4 Effect of reduction of DG capacity

If DG capacity decreases or some non-black start DGs are turned off, then the proposed method may need to enable DR on more buses through the optimal selection of controllable buses. In our case study, 2 non-black start DGs (DG3 and DG7) are turned off. According to the performed simulation for different numbers of controllable buses, as illustrated in Fig. 9, the overall restored

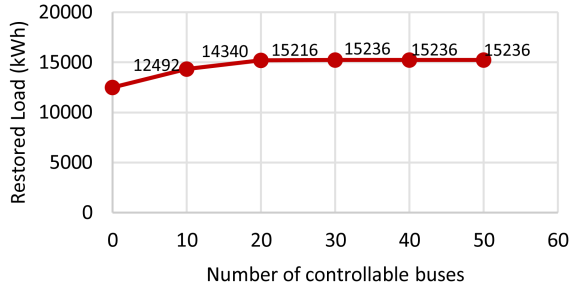

Fig. 8 *Energy restoration for non-black start generators turned off with different number of controllable buses*

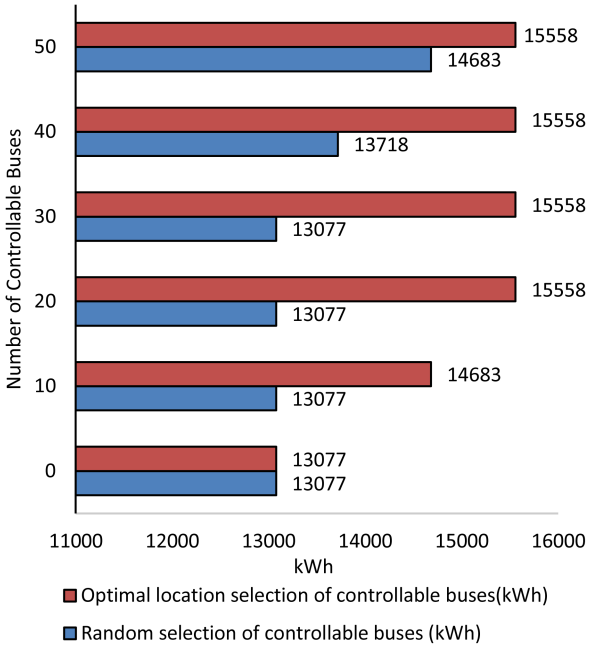

Fig. 9 *Restored energy comparison for optimal selection and random selection for a different number of controllable buses*

Table 3 Restored energy comparison for different controllable buses with the change of loads

Number of controllable buses	Restored energy, kWh
0	13,077
10	13,077
20	13,718
30	13,718
40	13,718
50	13,718

energy decreases due to the decrease in the amount of available generation, compared to Fig. 8. To deal with this scenario where less generation is available, more flexible loads are needed to be controlled to reduce the load demand. Therefore, the optimal controllable bus number increases from 20 to 30 in comparison with Table 3.

4.5 Effect in household-level demand

The optimal load profile defined from optimisation model 3.2 in a bus, are divided among the assigned houses considering their fixed and flexible load demands according to (30) and (31). Suppose after solving the optimization model 3.2, the target load at bus 16 is divided as local targets among 10 houses considering their flexible and fixed loads for each time. Fig. 10 shows one household load in bus 16. It illustrates that target load increases with time, as shown in Fig. 7. It also shows that the household load is reduced compared to the maximum load demand, which is a fixed load for the without DR method. To maintain this reduced load, flexible

© The Institution of Engineering and Technology 2019

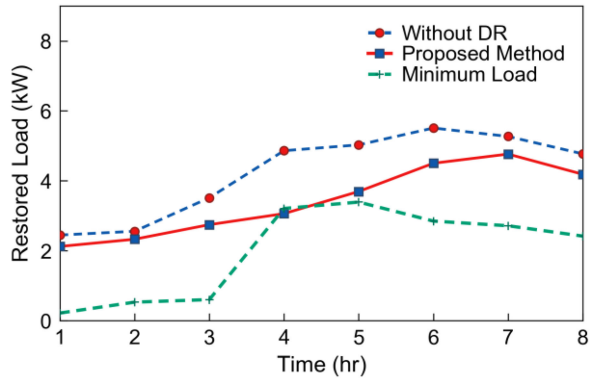

Fig. 10 *One household profile for the without DR and proposed methods at bus 16*

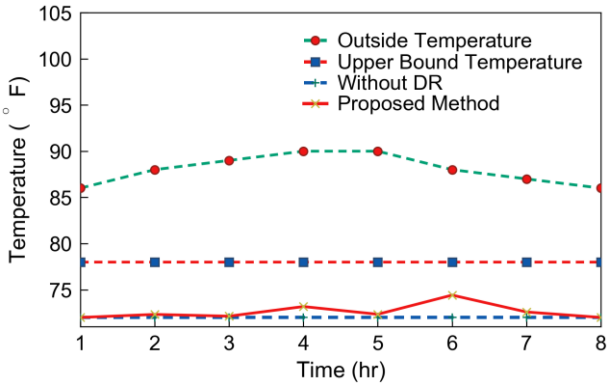

Fig. 11 *Outside and indoor temperatures for a house at bus 16 for different control methods*

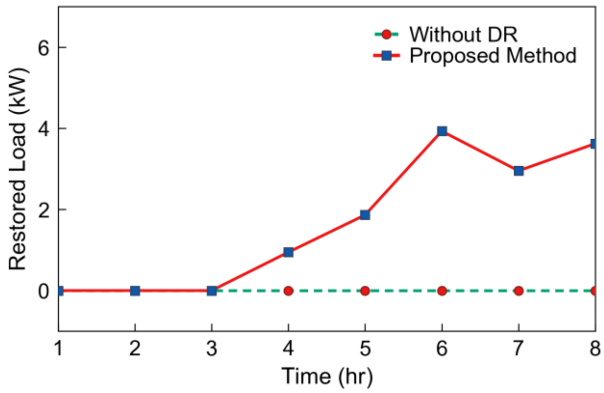

Fig. 12 *One household restored load profiles for the without DR and proposed methods at bus 87*

appliances are controlled using HEM. Due to space limitations, we decide to omit the scheduled load profiles of all appliances in this paper. Fig. 11 shows the only indoor temperature control through HEM. It shows that indoor temperature increases from 72°F compared to the without DR method for the proposed method to maintain the local target level of load. HEM maintains the comfortable temperature range up to 78°F.

Similarly, we can consider another household load for bus 87. Based on Figs. 5 and 6, bus 87 is not energised for the without DR method and is energised for the proposed method. Therefore, the household load is restored after 3 h based on our proposed method, but it does not have any restored load for the without DR method, as shown in Fig. 12. Figs. 10–12 show that our approach helps to restore energy in one house by reducing flexible load demand from another house, while ensuring comfort.

4.6 Effect of HEM in system resiliency

With the help of HEM, target loads in the household to bus levels are maintained. Impact of changing preferable load demand in HEM will impact the DSR. For instance, if AC loads are preferred to be controlled between 72 and 76°F instead of 72 and 78°F, then load requirement will increase for each house. The minimum load requirement of the buses will also be changed. This impact can be observed in Table 3. If the number of controllable buses is 10, then restored energy is only 13,077 kWh for 72–76°F preferable temperature range. It is 14,683 kWh for 72–78°F preferable temperature range according to Fig. 9. Restored energy also reduces from 15,558 kWh for 72–78°F to 13,718 kWh 72–76°F for optimal 20 controllable buses.

5 Conclusion

In this paper, we propose an innovative DR-based method for load restoration. The proposed method contains three-level hierarchical models formulated as three optimisation problems. Numerical results show that the load restoration performance can be significantly improved with the utilisation of DR in a distribution system with limited generation resources and microgrids facing multiple outages caused by natural disasters. Optimal allocation of controllable bus can further improve the restoration performance of the proposed method. Consideration of uncertainties in HEM system ensures maintaining the load level of the controlled buses. Overall, with the proposed method it is demonstrated that controlling the flexible loads in one house can help the DSR to pick up other fixed loads. Furthermore, the methods used here, such as assign time-varying load instead of spot load, define the feasible controllable range of load demand on a distribution bus, and maintain target load considering uncertainties in load demand and solar generation through HEM, can provide guidance on market design for DR when resilience is considered.

6 Acknowledgment

The work was supported by the U.S. Department of Energy Office of Electricity Delivery and Energy Reliability, Advanced Grid Research and Development. The submitted manuscript has been created by UChicago Argonne, LLC, Operator of Argonne National Laboratory (Argonne). Argonne, a U.S. Department of Energy Office of Science laboratory, was operated under contract no. DE-AC02-06CH11357.

7 References

[1] Ton, D.T., Wang, W.-T. P.: 'A more resilient grid', *IEEE Power Energy Mag.*, 2015, **13**, (3), pp. 26–34

[2] Gholami, A., Shekari, T., Amirioun, M. H., *et al.*: 'Towards a consensus on the definition and taxonomy of power system resilience', *IEEE Access*, 2018, **6**, pp. 32035–32053

[3] Gholami, A., Aminifar, F.: 'A hierarchical response-based approach to the load restoration problem', *IEEE Trans. Smart Grid*, 2017, **8**, (4), pp. 1700–1709

[4] Sharma, A., Kiran, D., Panigrahi, B.K.: 'Planning the coordination of overcurrent relays for distribution systems considering network reconfiguration and load restoration', *IET Gener. Transm. Distrib.*, 2017, **12**, (7), pp. 1672–1679

[5] Riahinia, S., Abbaspour, A., Aghtaie, M., *et al.*: 'Load service restoration in active distribution network based on stochastic approach', *IET Gener. Transm. Distrib.*, 2018, **12**, (12), pp. 3028–3036

[6] Nguyen, C.P., Flueck, A.J.: 'Agent based restoration with distributed energy storage support in smart grids', *IEEE Trans. Smart Grid*, 2012, **3**, (2), pp. 1029–1038

[7] Kim, Y., Wang, J., Lu, X.: 'A framework for load service restoration using dynamic change in boundaries of advanced microgrids with synchronous-machine DGs', *IEEE Trans. Smart Grid*, 2018, **9**, (4), pp. 3676–3790

[8] Kleinberg, M.R., Miu, K., Chiang, H.: 'Improving service restoration of power distribution systems through load curtailment of in-service customers', *IEEE Trans. Power Syst.*, 2011, **26**, (3), pp. 1110–1117

[9] Lei, S., Chen, C., Wang, J., *et al.*: 'Mobile emergency generator pre-positioning and real-time allocation for resilient response to natural disasters', *IEEE Trans. Smart Grid*, 2018, **9**, (3), pp. 2030–2041

[10] Li, J., Ma, X.Y., Liu, C.C., *et al.*: 'Distribution system restoration with microgrids using spanning tree search', *IEEE Trans. Power Syst.*, 2014, **29**, (6), pp. 3021–3029

[11] Ma, S., Su, L., Wang, Z., *et al.*: 'Resilience enhancement of distribution grids against extreme weather events', *IEEE Trans. Power Syst.*, 2014, **29**, (6), pp. 3021–3029

[12] Wang, Z., Shen, C., Xu, Y., *et al.*: 'Risk-limiting load restoration for resilience enhancement with intermittent energy resources', *IEEE Trans. Smart Grid*, 2019, **10**, (3), pp. 2507–2522

© The Institution of Engineering and Technology 2019

[13] Chen, C., Wang, J., Qiu, F., *et al.*: 'Resilient distribution system by microgrids formation after natural disasters', *IEEE Trans. Smart Grid*, 2016, **7**, (2), pp. 958–966
[14] Xu, Y., Liu, C.C., Schneider, K.P., *et al.*: 'Microgrids for service restoration to critical load in a resilient distribution system', *IEEE Trans. Smart Grid*, 2018, **9**, (1), pp. 426–437
[15] Yuan, W., Wang, J., Qiu, F., *et al.*: 'Robust optimization-based resilient distribution network planning against natural disasters', *IEEE Trans. Smart Grid*, 2016, **7**, (9), pp. 2817–2826
[16] Shi, D., Luo, Y., Sharma, R. K.: 'Active synchronization control for microgrid reconnection after islanding'. Proc. IEEE PES Innovative Smart Grid Technologies, Europe, Istanbul, Turkey, 2014, pp. 1–6.
[17] Chen, B., Chen, C., Wang, J., *et al.*: 'Multi-time step service restoration for advanced distribution systems and microgrids', *IEEE Trans. Smart Grid*, 2017, **9**, (6), pp. 6793–6805
[18] Wang, F., Chen, C., Li, C., *et al.*: 'A multi-stage restoration method for medium-voltage distribution system with DGs', *IEEE Trans. Smart Grid*, 2017, **8**, (6), pp. 2627–2636
[19] Gholami, A., Shekari, T., Grijalva, S.: 'Proactive management of microgrids for resiliency enhancement: an adaptive robust approach', *IEEE Trans. Sustain. Energy*, 2019, **10**, (1), pp. 470–480
[20] Chen, B., Chen, C., Wang, J., *et al.*: 'Sequential service restoration for unbalanced distribution systems and microgrids', *IEEE Trans. Power Syst.*, 2018, **33**, (2), pp. 1507–1520
[21] Shareef, H., Ahmed, M.S., Mohamed, A., *et al.*: 'Review on home energy management system considering demand responses, smart technologies, and intelligent controllers', *IEEE Access*, 2018, **6**, pp. 24498–24509
[22] Chen, S., Liu, C. C.: 'From demand response to transactive energy: state of the art', *J. Mod. Power Syst. Clean Energy*, 2017, **5**, (1), pp. 10–19
[23] Arun, S.L., Selvan, M.P.: 'Dynamic demand response in smart buildings using an intelligent residential load management system', *IET Gener. Transm. Distrib.*, 2017, **11**, (17), pp. 4348–4357
[24] Jay, D., Swarup, K.S.: 'Demand response based Automatic Generation Control in smart-grid deregulated market'. IEEE 6th Int. Conf. on Power System, New Delhi, India, 2016
[25] Wang, D., Ge, S., Jia, H., *et al.*: 'A demand response and battery storage coordination algorithm for providing microgrid tie-line smoothing services', *IEEE Trans. Sustain. Energy*, 2014, **5**, (2), pp. 476–486
[26] Wang, F., Zhou, L., Ren, H., *et al.*: 'Multi-objective optimization model of source–load–storage synergetic dispatch for a building energy management system based on TOU price demand response', *IEEE Trans. Ind. Appl.*, 2018, **54**, (2), pp. 1017–1028
[27] Huang, H., Li, F., Mishra, Y.: 'Modeling dynamic demand response using Monte Carlo simulation and interval mathematics for boundary estimation', *IEEE Trans. Smart Grid*, 2015, **6**, (6), pp. 2704–2713
[28] Reddy, S., Mukkapati, B., Panwar, L.K., *et al.*: 'Dynamic energy balancing cost model for day ahead markets with uncertain wind energy and generation contingency under demand response', *IEEE Trans. Ind. Appl.*, 2018, **54**, (5), pp. 4908–4916
[29] Chen, S., Chen, Q., Xu, Y.: 'Strategic bidding and compensation mechanism for a load aggregator with direct thermostat load control', *IEEE Trans. Smart Grid*, 2018, **9**, (3), pp. 2327–2336
[30] Qin, J., Wan, Y., Yu, X., *et al.*: 'Consensus-based distributed coordination between economic dispatch and demand response', *IEEE Trans. Smart Grid*, 2018, Early access
[31] Chen, Q., Zhao, X., Gan, D.: 'Active-reactive scheduling of active distribution system considering interactive load and battery storage'. *Prot. Control Mod. Power Syst.*, 2017, **2**, (29), pp. 1–11.
[32] Yu, R., Yang, W., Rahardja, S.: 'A statistical demand-price model with its application in optimal real-time price', *IEEE Trans. Smart Grid*, 2012, **3**, (4), pp. 1734–1742
[33] Medinal, J., Muller, N., Roytelman, I.: 'Demand response and distribution grid operations: opportunities and challenges', *IEEE Trans. Smart Grid*, 2010, **1**, (2), pp. 193–198
[34] Zheng, W., Wu, W., Zhang, B., *et al.*: 'Distributed optimal residential demand response considering operational constraints of unbalanced distribution networks', *IET Gener. Transm. Distrib.*, 2018, **12**, (9), pp. 1970–2979
[35] Syrri, A.L.A., Mancarella, P.: 'Reliability and risk assessment of post-contingency demand response in smart distribution networks', *Sustain. Energy, Grids Netw.*, 2016, **7**, pp. 1–12
[36] Chen, C., Wang, J., Kishore, S.: 'A distributed direct load control approach for large-scale residential demand response', *IEEE Trans. Power Syst.*, 2014, **29**, (5), pp. 2219–2228
[37] Hafiz, F., Queiroz, A.R., Husain, I.: 'Coordinated control of PEV and PV-based storage system under generation and load uncertainties'. Proc. IEEE Industry Application Society Annual Meeting, Ohio, Oct. 2018
[38] Hafiz, F., Queiroz, A.R., Husain, I.: 'Multi-stage stochastic optimization for a PV-storage hybrid unit in a household'. Proc. IEEE Industry Application Society Annual Meeting, Ohio, Oct. 2017
[39] Infanger, G., Morton, D.P.: 'Cut sharing for multistage stochastic linear programs with interstage dependency', *Math. Program.*, 1996, **75**, (2), pp. 241–256
[40] de Queiroz, A. R., Morton, D. P.: 'Sharing cuts under aggregated forecasts when decomposing multi-stage stochastic programs', *Oper. Res. Lett.*, 2013, **41**, (3), pp. 311–316
[41] Hafiz, F., Queiroz, A.R., Husain, I., *et al.*: 'Energy management and optimal storage sizing for a shared community: a multi-stage stochastic approach', *Appl. Energy*, 2019, **236**, (15), pp. 42–54
[42] 'Household load and solar generation data', 2016. Available at http://www.pecanstreet.org
[43] 'Historical weather data', 2016. Available at http://www.w2.weather.gov
[44] 'IEEE PES distribution test feeders', 2014. Available at http://www.ewh.ieee.org/soc/pes/dsacom/testfeeders/index.html

© The Institution of Engineering and Technology 2019